Titanate Nanosheets as High Refractive Layer in Vertical Microcavity Incorporating Semiconductor Quantum Dots

ARTICLE *in* THE JOURNAL OF PHYSICAL CHEMISTRY C · OCTOBER 2010

Impact Factor: 4.77 · DOI: 10.1021/jp106951y

7 AUTHORS, INCLUDING:

Massimo Guglielmi
University of Padova
238 PUBLICATIONS **4,138** CITATIONS
SEE PROFILE

Valentina Bello
University of Padova
63 PUBLICATIONS **704** CITATIONS
SEE PROFILE

Alessandro Chiasera
Italian National Research Council
239 PUBLICATIONS **2,235** CITATIONS
SEE PROFILE

Maurizio Ferrari
Italian National Research Council
522 PUBLICATIONS **5,505** CITATIONS
SEE PROFILE

Titanate Nanosheets as High Refractive Layer in Vertical Microcavity Incorporating Semiconductor Quantum Dots

Alessandro Antonello,[†] Massimo Guglielmi,[†] Valentina Bello,[‡] Giovanni Mattei,[‡] Alessandro Chiasera,[§] Maurizio Ferrari,[§] and Alessandro Martucci*[,†]

INSTM, Dipartimento di Ingegneria Meccanica Settore Materiali, Università di Padova, via Marzolo 9, 35131 Padova, Italy, CNISM, Dipartimento di Fisica, Università di Padova, via Marzolo 8, 35131 Padova, Italy, and CNR-IFN Istituto di Fotonica e Nanotecnologie, CSMFO Lab, via alla Cascata 56/C, Povo 38123 Trento, Italy

Received: July 26, 2010

The use of titanium dioxide as the high refractive index component in optical structures is very attractive because of its optical properties. In this work, we developed a novel synthesis of colloidal layered titanate consisting of nanosheets of titanium oxide. A colloidal solution of titanate nanosheets was deposited by spin coating and treated by thermal annealing and UV irradiation, obtaining high refractive index thin films. Transmission electron microscopy, X-ray diffraction, and spectroscopic ellipsometry were used to characterize titanate powders and the evolution of titanate films under the employed treatments. The developed low temperature UV-assisted titanate processing was found to be suitable in the fabrication of multilayer dielectric Bragg mirrors, which can be used in a vertical optical microcavity incorporating CdSe@ZnS quantum dots (QDs) in the defect layer. The developed fabrication procedure did not result in the loss of QDs emission properties, allowing for optical characterization of the coupling between QDs emission and the cavity. The compatibility between the processing of high refractive index materials and QDs functionality is very promising for novel strategies in the fabrication of optically active photonic structures.

Introduction

The possibility to process high refractive index materials in the presence of photoluminescence (PL) active species without damaging their properties is essential for the successful realization of optically active photonic structures.

In this work, we describe a convenient strategy for the processing of materials based on titanium oxide and semiconductor quantum dots (QDs). As an example of potential application, the developed procedure was applied to the fabrication of a vertical microcavity embedding QDs in the defect layer.

Titanium dioxide is among the most studied materials due to photochemical, electronic, and optical properties, which make it an interesting material for solar cells, photocatalytic purposes, antireflection coatings, and distributed Bragg reflectors (DBRs). It has been widely studied for optical applications because of its transparency in the visible spectral region, UV absorption properties, and high refractive index, and a wide range of processing methods have been so far developed. In particular, colloidal syntheses allow for nanometric particles, which can be used for functional nanocomposites,[1−8] high refractive index materials to be used in optical devices, and materials with controlled morphology and porosity in the nanometer scale with large surface area.[9−14] All common titania polymorphs have been obtained by colloidal routes tailoring compositional and processing parameters.[15−21]

More recently, layered titanates have been extensively studied as novel precursors for titania with controlled morphology and crystalline structure.[22−27] These compounds are very attractive due to optical, photochemical, and electronic properties. In addition, ion-exchange and intercalation of functional organic molecules can be applied to such materials.[28−41] Layered titanates can also be modified by UV irradiation, which has been shown to be a useful alternative to thermal treatment to obtain well-densified material with high refractive index.[42−44]

The high flexibility and wide range of processing conditions of titanate-based materials attracted our attention for optically active devices fabrication.

In the following, a synthetic procedure has been developed to obtain a transparent colloidal solution of titanate nanosheets, which were applied to film deposition and fabrication of an optically active vertical optical microcavity.

The effect of heat treatment and UV irradiation has been studied and used for the enhancement of the refractive index. Film structure evolution was followed by XRD and spectroscopic ellipsometry.

The developed material processing has been found to be suitable for the preparation of DBRs mirrors. These could be used in the fabrication of a Fabry−Perot optical microcavity incorporating luminescent CdSe−ZnS quantum dots (QDs) in the defect layer. Quantum dots are very promising as photoluminescence (PL) emitters due to high stability and PL quantum yield along with largely tunable emission and absorption properties with particles size. Furthermore, a lot of colloidal chemistry methods have been developed for the obtainment of stable core−shell heterostructures.

The coupling of QDs emission with photonic structures of different types has been studied in previous works,[46−48] and the related possibility of efficiently manipulating the QDs spontaneous emission is very attractive.

The optical structure here presented was entirely realized by spin coating deposition. The adopted multistack fabrication did not result in loss of QDs photoluminescence, allowing for optical

* Corresponding author. E-mail: alex.martucci@unipd.it.
[†] INSTM, Università di Padova.
[‡] CNISM, Università di Padova.
[§] CNR-IFN Istituto di Fotonica e Nanotecnologie.

10.1021/jp106951y
Published on Web 10/07/2010

characterization of the coupling between QDs emission and optical cavity.

Experimental Procedures

Materials. Titanium tetraisopropoxide ($Ti(OPr^i)_4$), ethylene glycol (EG), tetramethylammonium hydroxide (TMA), cadmium oxide, zinc oxide, oleic acid, diisooctylphosphinic acid, octadecylammine, octadecene, elemental selenium, elemental sulfur, and all employed solvents were purchased from Aldrich. Doubly distilled water was used in the reactions.

Titanate Nanosheets Synthesis. Titanate nanosheets were synthesized from EG, $Ti(OPr^i)_4$, water, and TMA. 107 mmol of EG was heated on a heating mantle in a 50 mL three-necked flask fitted with a refluxing condenser at 60 °C under vacuum for 20 min. Subsequently, the temperature was raised to 110 °C after switching to nitrogen flow. Twelve millimoles of $Ti(OPr^i)_4$ was injected, and the solution turned immediately opaque. A second injection consisting of 9 mmol of TMA dissolved in 300 mmol of water was quickly performed, and an optically clear solution was obtained within a few seconds. The synthesis was carried out at 110 °C reaction temperature for 4 h.

Titanate nanosheets were precipitated by addition of acetone and collected by centrifugation at 4000 rpm for 4 min. The obtained powder was washed two times with acetone and two times with methanol and dried under vacuum.

Titanate Film Treatments and Optical Microcavity Fabrication. The powders obtained as described above were first dispersed in a 0.03 M TMA aqueous solution, obtaining a clear colloidal solution with a concentration of 200 g/mL. This solution was 2-fold diluted with methanol and deposited on quartz and silicon substrates by spin coating at 3000 rpm for 20 s.

Films were first stabilized at 100 °C for 15 min and then annealed at 200 or 500 °C for 1 h in air (labeled as **100**, **200**, and **500**, respectively) or irradiated by UV light for 15 min (labeled as **UV**).

The combined effect of UV irradiation and subsequent thermal annealing at 200 °C was also analyzed. These samples will be indicated as **UV+200**. A treatment analogous to **UV+200** but reducing both UV and thermal treatment time to 5 min was also adopted. This procedure will be denoted as **UV+200b**.

Bragg gratings were grown on quartz substrates by alternatively depositing titanate and silica films up to 6 couples. Silica sol was obtained from conventional sol−gel processing of tetraethoxysilane following the method described by Fardad et al.[49]

Two procedures were adopted for gratings fabrication. The first, **grating a**, consists of annealing each layer at 500 °C for 15 min, while the second, **grating b**, involves the **UV+200b** treatment of the titanate layer and 5 min thermal annealing at 200 °C for the SiO_2 layer.

The gratings were designed to have a quarter wave thickness and a maximum reflectivity at 620 nm. Because the refractive index of SiO_2 was measured to be 1.44 independently of the annealing temperature, the target SiO_2 layer thickness was 108 nm. The titanate layers deposition was optimized to have a layer thickness of 67 and 69 nm for **grating a** and **grating b**, respectively, because in this case the refractive index depends on the specific film treatment, as explained in the following.

The Fabry−Perot optical microcavity was realized in three stages. First, **grating a** was grown on a quartz substrate, and then a QDs-loaded ZrO_2 defect layer was deposited by spin coating. Finally, **grating b** was deposited to complete the microcavity.

Both **grating a** and **grating b** DBR mirrors were separately grown on a quartz substrate for optical characterization.

The defect layer was prepared by a procedure analogous to that described by Jaseniak et al.[50] A sol−gel solution prepared by mixing zirconium isopropoxide and acetylacetone in isopropanol was mixed with a colloidal solution of 6-amino-1-hexanol functionalized CdSe−CdS−ZnS core−shell nanoparticles in ethanol.

CdSe−CdS−ZnS QDs were synthesized using CdSe nanocrystals obtained as described by Van Embden et al.,[51] while the shell was grown adopting a procedure similar to that described in recent works.[52−54]

The defect layer was deposited in three successive depositions with a heat treatment at 250 °C for 5 min each. The final film thickness was designed to be one-half of the QDs PL peak wavelength to guarantee good overlapping between QDs PL emission and the cavity mode. As the emission wavelength was 620 nm and the refractive index of the ZrO_2-QDs films was measured to be 1.76, the spin coating parameters were optimized to have a defect layer thickness of 176 nm.

Characterization. Titanate powders and thin films have been characterized by X-ray diffraction (XRD) using a Philips PW1710 diffractometer equipped with grazing-incidence optics. The analysis was performed using CuK_α Ni filtered radiation at 30 kV and 40 mA.

Transmission electron microscopy (TEM) measurements were performed on a FEI-Tecnai field-emission gun (FEG) (S)TEM F-20 Super Twin, at 200 kV primary tension. Analyses were performed on dried-powder dispersed in methanol and deposited on a holey carbon film supported by a copper grid.

Spectroscopic ellipsometry analyses were done with a VASE32 J. A. Wollam Co. Measurements have been performed at 65° and 75° with 10 nm wavelength step in the 300−1000 nm range. Transmission spectra were also taken and used for optical modeling along with the ellipsometry data.

The ellipsometry setup has also been used to collect specular reflectance spectra. Because of the physical limitation of the instrument, only reflection at angles larger than 15° could be measured.

UV−vis−NIR transmission spectra were taken using a JASCO V-570 spectrometer equipped with an integrating sphere (model ISV-469, internally coated with barium sulfate). Reflectance spectra could be taken at almost normal reflection angle using the integrating sphere apparatus.

Infrared spectroscopy (FT-IR) measurements were performed in the 400−4000 cm^{-1} range using a JASCO FT-IR 6300 system.

UV irradiation of titanate films was performed with a mercury−xenon lamp (Hamamatsu LC6) with an intensity of about 460 mW/cm^2 at 365 nm.

Luminescence emission of QDs in the cavity was characterized using the 514.5 nm line of an Ar^+ ion laser as excitation source. This was focused at 2° incident angle on the sample from the quartz substrate side of the multilayer structure, while the cavity emission was detected at different angles from the opposite side.

Results and Discussion

Colloidal Titanate Nanosheets. Figure 1 shows the XRD pattern of the titanate nanosheets powder. Strong diffraction peaks in the low angle region are present, suggesting a layered

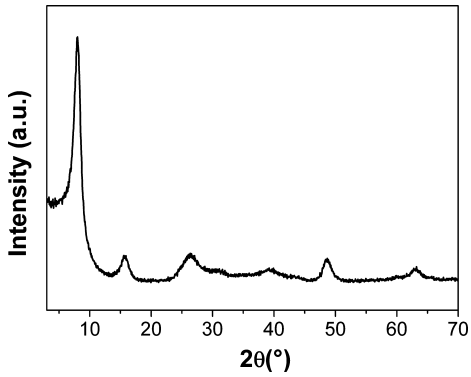

Figure 1. XRD diffraction pattern of vacuum-dried titanate powders.

structure where titanate sheets are orderly stacked. Similar data have been reported by Ohya et al.,[23] where TMA and $Ti(OPr^i)_4$ were used as precursors. Peaks at 7.7° and 15.5° can be attributable to first- and second-order diffraction from the layer stack periodicity. Additionally, an interlayer distance of 1.14 nm can be retrieved from the peak position, and a layers stack length of 4.4 nm can be estimated from peak width by applying the Scherrer relationship. This corresponds to about 4 orderly stacked titanate nanosheets.

The diffraction peaks at wider diffraction angle may arise from the in-plane crystallinity of each layer and from the particular stacking arrangement assumed by the titanates.[26,27] Portehault et al.[27] assigned a pseudolepidocrocite structure to layered titanates synthesized under nonaqueous conditions. The XRD pattern obtained in that work is very similar to that shown in Figure 1, suggesting a pseudolepidocrocite structure also in our case.

The layered structure is also evident from TEM analysis shown in Figure 2. The interlayer distance and number of stacked layer are in good agreement with those estimated from XRD measurements. The lateral dimension of the titanate layer is about 5 nm, confirming the nanometric dimension of these nanostructures.

When this powder is dispersed in water with the addition of TMA, it is likely that layered titanates are in an exfoliated state, where they exist as single sheets, as observed by Sasaki et al.[26]

Thin Film Treatments. In Table 1, refractive indexes, interlayer distances, and thickness contraction with respect to the **100** sample are reported for all employed processing conditions.

TABLE 1: Refractive Indexes at 630 nm, Film Thickness Contraction with Respect to 100 Sample, and Interlayer Distances (*d*) Estimated from XRD Peak Position of Titanate Films under Varying Processing Conditions

sample	refractive index	thickness contraction (%)	*d* (nm)
100	1.83	0	1.14
UV	2.15	39	0.93
200	2.03	24	1.14
UV+200	2.28	57	0.69
UV+200b	2.26	54	0.71[a]
500	2.30	59	—[b]

[a] **UV+200b** sample does not show the same structure in the whole film as explained in the text. The reported distance refers to the fully treated structure. [b] **500** sample is in the anatase structure.

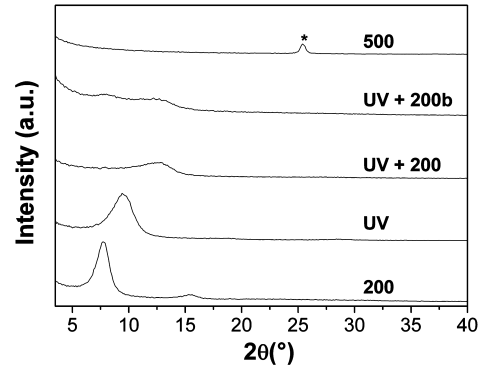

Figure 3. XRD patterns of the titanate films under UV and thermal treatment ((101) anatase diffraction peak is indicated by *).

In Figure 3, XRD patterns of titanate films under different treatments are reported, and FT-IR spectra of selected titanate films are shown in Figure 4.

Comparing the XRD pattern of titanate powders (Figure 1) with the patterns of titanate films (Figure 3), it can be seen that the layered structure is unaffected after thermal annealing at 200 °C (**200** pattern). The FT-IR analyses (see Figure 4) demonstrated the presence of tetramethylammonium in the **200** samples, which is most likely intercalated between the titanate layers. A layer thickness contraction is observed (see Table 1), which is related to evaporation of solvents still remaining after drying at 100 °C. This also explains the rise of refractive index observed from **100** to **200** samples.

The XRD pattern of **200** sample (see Figure 3) does not show the diffraction peak at wider angle detected in the XRD powder

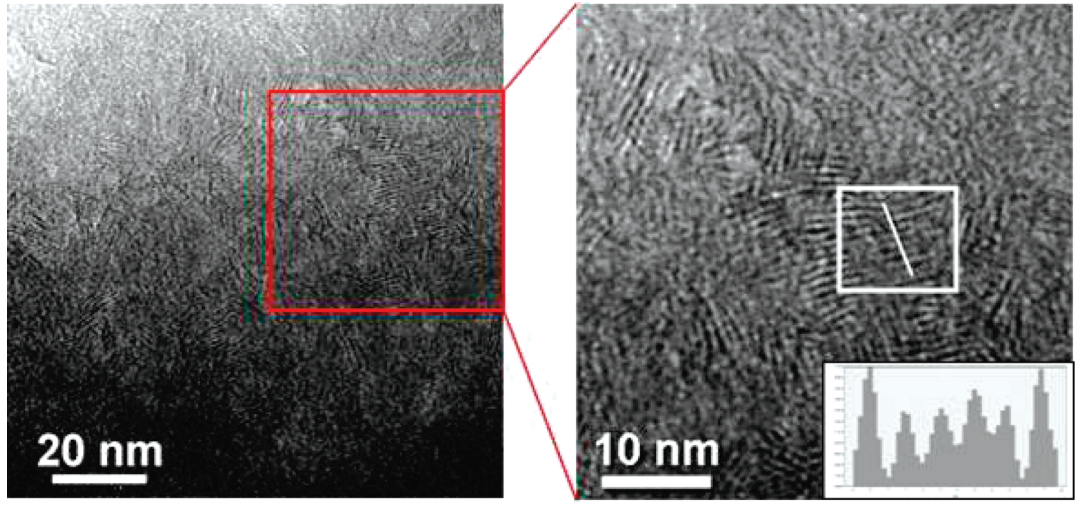

Figure 2. TEM (a) and HR-TEM (b) image of synthesized layered titanates. The intensity profile along the white line is also reported.

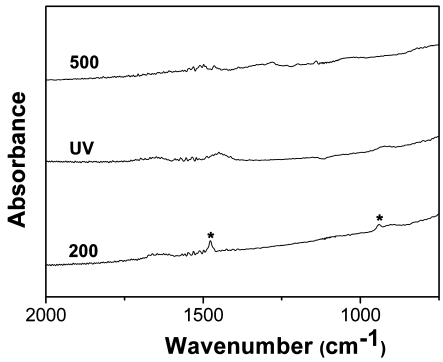

Figure 4. FT-IR spectra of selected titanate film (*: TMA vibration band).

pattern (see Figure 1). This suggests a preferential orientation of the nanosheets when deposited on a substrate, as observed in other works,[23] with the stacking direction mostly oriented perpendicularly to the substrate.

The interlayer diffraction peak positions and widths are unchanged when comparing XRD powder and film patterns, implying no influence of the spin coating process on the titanate layer arrangement.

UV irradiation has a considerable effect on film structure, as observed in other works for analogous materials.[42−44] The **UV** sample presents an interlayer distance contraction with respect to the **200** sample, and the diffraction peak is wider (see Table 1 and Figure 3). In addition, no FT-IR peaks of TMA can be detected (see Figure 4).

These results are explained considering the photocatalytic properties of titanate sheets[42−44] resulting in the decomposition under UV irradiation of the intercalated TMA organic cations. The removal of the organic molecules from the interlayer space induces the observed interlayer distance and thickness contraction, as well as enhancement of the refractive index and partial loss of the stack order as evidenced from XRD peak broadening.[45]

The densification is nonetheless not complete after UV treatment. This is clearly observed from the XRD pattern of the **UV+200** sample (see Table 1 and Figure 3) where further contraction of the layered structure to very small interlayer distances is accompanied by a strong loss of stacking order, as deduced from the large peak broadening. This can be caused by a thermally activated removal of photodecomposition byproducts still present between the layers, leading to a more compact structure. It is worth noting that the thickness contraction and refractive index are largely increased with respect to the **UV** sample, leading to values that approach those of samples annealed at 500 °C (see Table 1).

The influence of processing parameters, such as UV irradiation and thermal annealing time, has been further analyzed. It was found that 5 min of UV irradiation followed by 5 min at 200 °C (**UV+200b** treatment) were sufficient to reach a refractive index of 2.26 (Table 1), almost equal to that of **UV+200** samples, even if the XRD pattern still evidenced the presence of diffraction signal belonging to pristine interlayer distance (Figure 1). It is likely that the bottom part of the film is not completely treated because UV light is strongly attenuated. Longer UV exposures are thus required to achieve a homogeneous structure in the whole film.

The thermal treatment at 500 °C induces a high degree of layer contraction and densification due to thermal decomposition and elimination of TMA molecules and formation of the anatase

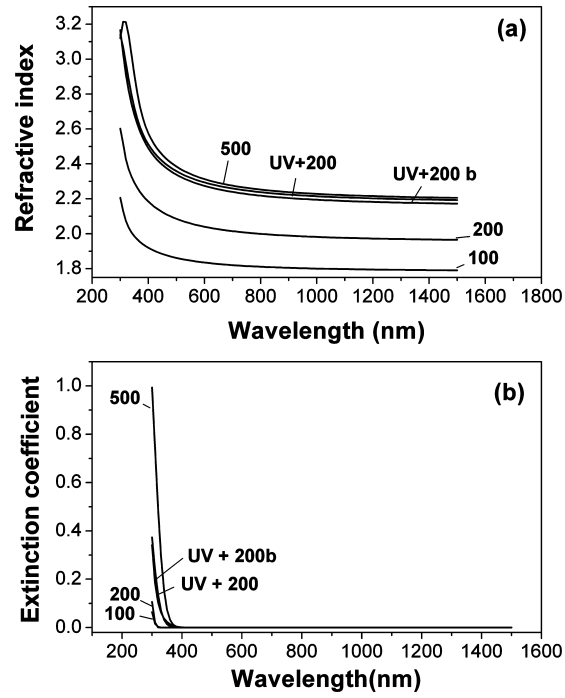

Figure 5. Refractive index (a) and extinction coefficient (b) curves of selected films.

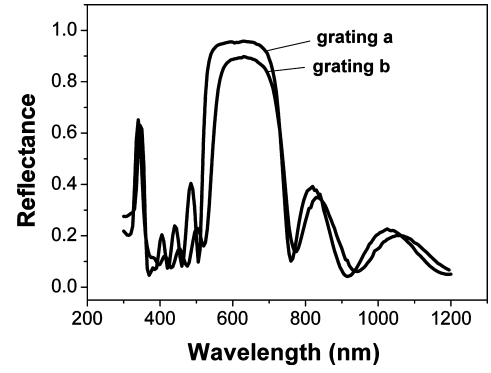

Figure 6. Reflectance spectra of **grating a** and **grating b**.

crystal structure, as shown in Figures 3 and 4. This in turn causes the high refractive index values obtained in the **500** sample (see Table 1).

The effect of the developed treatments on optical constants is summarized in Figure 5, where refractive index and extinction coefficient curves are reported.

It is apparent that **UV+200** or **UV+200b** give almost the same refractive index as thermal annealing at 500 °C. The extinction coefficient increases upon thermal or UV treatments in the 300−400 nm range, which is the typical titanate or TiO_2 absorption region.

The extinction coefficient is related to the volume concentration of absorbing species.[55] Thus, the increase of the k value observed for the **UV+200** or **UV+200b** sample, with respect to the k value of the **100** or **200** sample, is in agreement with the interlayer distance contraction and the consequent increase in titanate sheet volume concentration.

Layered titanates have been shown to have a blue-shifted absorption onset with respect to anatase titania.[39−41] The extinction coefficient curves reported in Figure 5b confirm this shift; in fact, the **500** films are crystalline anatase, while the other samples are made of titanate layers. Also, optical absorption measurements on the colloidal titanate solution confirm this feature (data not shown).

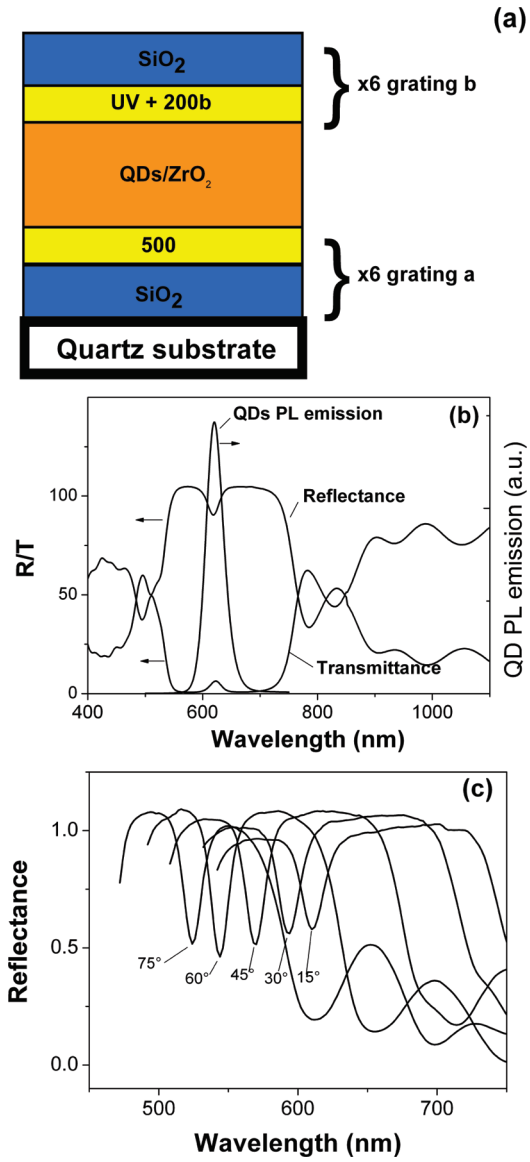

Figure 7. (a) Schematic representation of the fabricated optical microcavity; (b) transmittance and reflectance spectra taken with an integrating sphere and PL emission of QDs in ZrO_2 matrix; and (c) specular reflectance spectra of the resulting structure at varying reflection angles.

Optical Microcavity. The reflectance spectra of DBRs grown on quartz substrates are shown in Figure 6. Both **grating a** and **grating b** show a maximum reflectance of 0.95 and 0.9, respectively, centered at 620 nm.

The higher reflectance of **grating a** is due to the higher refractive index of titanate film treated at 500 °C.

Measured reflectance values are lower than those retrieved from simulations (0.99 and 0.98 for **grating a** and **grating b**, respectively). This is likely due to surface quality of the deposition that must be improved to increase specular reflection and to differences between target and obtained film thicknesses.

The two gratings were used in the microcavity structure represented in Figure 7a. Because of higher reflectance and complete stabilization of the titanate layers, the use of **grating a** would have been desirable for both mirrors. On the other hand, annealing of the structure at 500 °C after the deposition of the QDs-ZrO_2 defect layer would have resulted in the degradation of QDs, which were shown to lose their emission properties at an annealing temperature above 300 °C.[44]

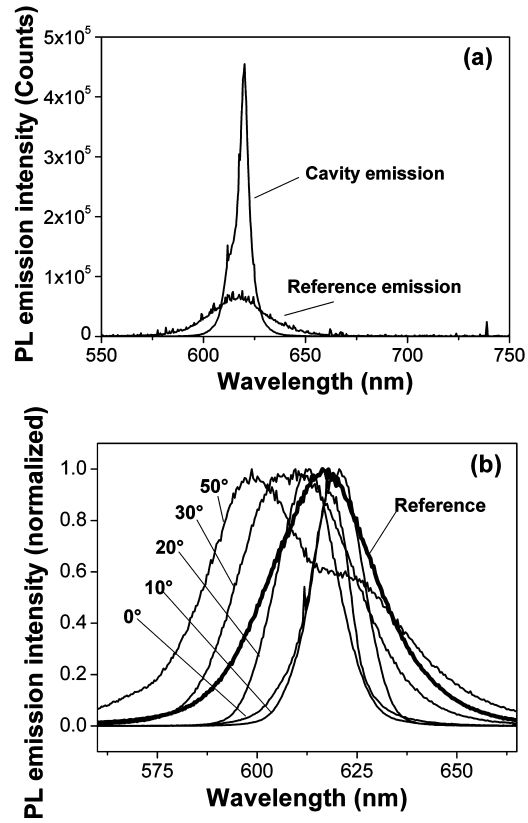

Figure 8. Emission of the cavity and of a neat QDs-ZrO_2 reference film under 514.5 nm laser excitation (a) and cavity emission under varying detection angle (b).

This motivated us to use the **UV+200b** treatment to achieve high refractive index, which enabled us not to exceed 200 °C treatment temperature and to minimize the annealing time. So, **grating b** was used to complete the microcavity.

The presence of the optical cavity is apparent in the transmittance and reflectance spectra of the resulting structure (Figure 7b). The quality factor Q (calculated as $\lambda/\Delta\lambda$, with λ and $\Delta\lambda$ being the cavity mode position and width, respectively) retrieved from these data is 31, and a good overlap with the spontaneous emission of QDs in ZrO_2 matrix was obtained. As expected, the angular dependence of the cavity position moves toward shorter wavelengths with increasing reflection angle (Figure 7c).

The PL emission of QDs was retained after the employed fabrication process, and the optical characterization of the coupling between QDs emission and the cavity was carried out. In Figure 8a, the spontaneous emission of the QDs inside the cavity is shown with the emission of a neat QDs-ZrO_2 reference film on quartz substrate with the same thickness of the defect layer in the cavity.

The modification of the emission profile is apparent in both the narrowing of the spectral line width and the spectral enhancement of cavity emission at normal detection direction (see Figure 8a). These observations are indicative of the coupling between the cavity and the QDs emission. The enhancement of the emission relative to the peak cavity is measured to be about 7, and it can be explained by the Purcell effect.[56] The influence of the cavity on the QDs spontaneous emission was further put in evidence by varying the PL detection angle. The results, summarized in Figure 8b, show the expected shift at lower wavelengths of the PL maximum with increasing departure from the normal direction. Uncoupled emission is seen at 50°

detection angle, likely due to gratings imperfections arising during DBR fabrication.

Even if optimization of the fabrication procedure is required to get higher *Q* values and better overall structure quality, these results show the advantage of using low temperature curable titanate film in photonic structure, where high refractive index materials are required. This permits one to extend the range of processing conditions to include the use of active specie, such as QDs, without destroying their peculiar properties.

Conclusions

The synthesis and characterization of a colloidal layered titanate nanosheets have been presented.

Transparent colloidal titanate solution could be spun to obtain thin films whose structural evolution under thermal and UV treatments could be followed by XRD, TEM, and ellipsometry measurements.

Low temperature titanate processing assisted by UV irradiation has been developed, which allowed one to obtain high refractive index films.

The processing flexibility of the colloidal titanates has been exploited for the fabrication of optical structures such as DBRs mirrors and vertical coplanar microcavities. QDs have been introduced in the defect layer of the optical cavity without loss of their emission properties, allowing for optical characterization of the cavity-QDs emission coupling.

Acknowledgment. This work has been supported by the EU commission through the 6FP "MULTIPRO" project.

References and Notes

(1) Wang, B.; Wilkes, G. L.; Hedrick, J. C.; Liptak, S. C.; McGrath, J. E. *Macromolecules* **1991**, *24*, 3449.
(2) Lee, L. H.; Chen, W. C. *Chem. Mater.* **2001**, *13*, 1137.
(3) Oliveira, P. W.; Krug, H.; Frantzen, A.; Mennig, M.; Schmidt, H. *SPIE Proc.* **1997**, *3136*, 452.
(4) Convertino, A.; Leo, G.; Tamborra, M.; Sciancalepore, C.; Striccoli, M.; Curri, M. L.; Agostiano, A. *Sens. Actuators, B* **2007**, *126*, 138.
(5) Nussbaumer, R. J.; Caseri, W.; Tervoort, T.; Smith, P. *J. Nanopart. Res.* **2002**, *4*, 319.
(6) Nussbaumer, R. J.; Caseri, W. R.; Smith, P.; Tervoort, T. *Macromol. Mater. Eng.* **2003**, *288*, 44.
(7) Yuwono, A. H.; Xue, J.; Wang, J.; Elim, H. I.; Ji, W.; Li, Y.; White, T. J. *J. Mater. Chem.* **2003**, *13*, 1475.
(8) Liu, Y. F.; Lu, C. L.; Li, M. J.; Zhang, L.; Yang, B. *Colloids Surf., A* **2008**, *328*, 67–72.
(9) Rabaste, S.; Bellessa, J.; Brioude, A.; Bovier, C.; Plenet, J. C.; Brenier, R.; Marty, O.; Mugnier, J.; Dumas, J. *Thin Solid Films* **2002**, *416*, 242.
(10) Almeida, R. M.; Gonçalves, M. C.; Portal, S. *J. Non-Cryst. Solids* **2004**, *345&346*, 562.
(11) Yoon, J.; Leea, W.; Caruge, J. M.; Bawendi, M.; Thomas, E. L.; Kooi, S.; Prasad, P. N. *Appl. Phys. Lett.* **2006**, *88*, 091102.
(12) Chiasera, A.; Belli, R.; Bhaktha, S. N. B.; Chiappino, A.; Ferrari, M.; Jestin, Y.; Moser, E.; Righini, G. C.; Tosello, C. *Appl. Phys. Lett.* **2006**, *89*, 171910.
(13) Rabaste, S.; Bellessa, J.; Bonnand, C.; Plenet, J.; Spanhel, L. *Eur. Phys. J. B* **2004**, *42*, 47.
(14) Poitras, C. B.; Lipson, M.; Du, H.; Hahn, M. A.; Krauss, T. D. *Appl. Phys. Lett.* **2003**, *82*, 4032.
(15) Yin, H.; Wada, Y.; Kitamura, T.; Kambe, S.; Murasawa, S.; Mori, H.; Sakata, T.; Yanagida, S. J. *J. Mater. Chem.* **2001**, *11*, 1694.
(16) Pottier, A.; Chanéac, C.; Tronc, E.; Mazerolles, L.; Jolivet, J. *J. Mater. Chem.* **2001**, *11*, 1116.
(17) Chatry, M.; Henry, M.; In, M.; Sanchez, C.; Livage, J. *J. Sol-Gel Sci. Technol.* **1994**, *1*, 233.
(18) Yanagisawa, K.; Ovenstone, J. *J. Phys. Chem. B* **1999**, *103*, 7781.
(19) Cheng, H.; Ma, J.; Zhao, Z.; Qi, L. *Chem. Mater.* **1995**, *7*, 663.
(20) Bhave, R. C.; Lee, B. I. *Mater. Sci. Eng., A* **2007**, *467*, 146.
(21) Lee, B. I.; Wang, X.; Bhave, R.; Hu, M. *Mater. Lett.* **2006**, *60*, 1179.
(22) Feist, T. P.; Davies, P. K. *J. Solid State Chem.* **1992**, *101*, 275.
(23) Ohya, T.; Nakayama, A.; Ban, T.; Ohya, Y.; Takahashi, Y. *Chem. Mater.* **2002**, *14*, 3082.
(24) Sasaki, T.; Watanabe, M.; Michiue, Y.; Komatsu, Y.; Izumi, F.; Takenouchi, S. *Chem. Mater.* **1995**, *7*, 1001.
(25) Gao, T.; Fjellv, T.; Norby, P. *Chem. Mater.* **2009**, *21*, 3503.
(26) Sasaki, T.; Watanabe, M.; Hashizume, H.; Yamada, H.; Nakazaw, H. *J. Am. Chem. Soc.* **1996**, *118*, 8329.
(27) Portehault, D.; Giordano, C.; Sanchez, C.; Antonietti, M. *Chem. Mater.* **2010**, *22*, 2125.
(28) Sasaki, T.; Watanabe, M. *J. Am. Chem. Soc.* **1998**, *120*, 4682.
(29) Yuan, Z. Y.; Su, B. L. *Colloids Surf., A* **2004**, *241*, 173.
(30) Sasaki, T.; Nakano, S.; Yamauchi, S.; Watanabe, M. *Chem. Mater.* **1997**, *9*, 602.
(31) Sasaki, T.; Komatsu, Y.; Fujiki, Y. *Chem. Mater.* **1992**, *4*, 894.
(32) Kotov, N. A.; Meldrum, F. C.; Fendler, J. H. *J. Phys. Chem.* **1994**, *98*, 8827.
(33) Xu, X. G.; Ding, X.; Chen, Q.; Peng, L. M. *Phys. Rev. B* **2006**, *73*, 165403.
(34) Riss, A.; Elser, M. J.; Bernardi, J.; Diwald, O. *J. Am. Chem. Soc.* **2009**, *131*, 6198.
(35) Miyamoto, N.; Kuroda, K.; Ogawa, M. *J. Mater. Chem.* **2004**, *14*, 165.
(36) Choy, J. H.; Lee, H. C.; Jung, H.; Kim, H.; Boo, H. *Chem. Mater.* **2002**, *14*, 2486.
(37) Umemura, Y.; Shinohara, E.; Koura, A.; Nishioka, T.; Sasaki, T. *Langmuir* **2006**, *22*, 3870.
(38) Jang, J. H.; Jeon, K. S.; Oh, S.; Kim, H. J.; Asahi, T.; Masuhara, H.; Yoon, M. *Chem. Mater.* **2007**, *19*, 1984.
(39) Sasaki, T.; Watanabe, M. *J. Phys. Chem. B* **1997**, *101*, 10159.
(40) Sato, H.; Ono, K.; Sasaki, T.; Yamagishi, A. *J. Phys. Chem. B* **2003**, *107*, 9824.
(41) Sakai, N.; Ebina, Y.; Takada, K.; Sasaki, T. *J. Am. Chem. Soc.* **2004**, *126*, 5851.
(42) Sasaki, T.; Ebina, Y.; Fukuda, K.; Tanaka, T.; Harada, M.; Watanabe, M. *Chem. Mater.* **2002**, *14*, 3524.
(43) Ohya, T.; Nakayama, A.; Ban, T.; Ohya, Y.; Takahashi, Y. *Bull. Chem. Soc. Jpn.* **2003**, *76*, 429.
(44) Abe, R.; Shinohara, K.; Tanaka, A.; Hara, M.; Kondo, J. N.; Domen, K. *Chem. Mater.* **1998**, *10*, 329.
(45) Sasaki, T.; Ebina, Y.; Tanaka, T.; Harada, M.; Watanabe, M. *Chem. Mater.* **2001**, *13*, 4661.
(46) Jasieniak, J.; Sada, C.; Chiasera, A.; Ferrari, M.; Martucci, A.; Mulvaney, P. *Adv. Funct. Mater.* **2008**, *18*, 3772.
(47) Lodahl, P.; van Driel, A. F.; Nikolaev, I. S.; Irman, A.; Overgaag, K.; Vanmaekelbergh, D.; Vos, W. L. *Nature* **2004**, *430*, 654.
(48) Ganesh, N.; Zhang, W.; Methias, P. C.; Chow, E.; Soares, J. A. N. T.; Malyarchuk, V.; Smith, A. D.; Cunningham, B. T. *Nat. Nanotechnol.* **2007**, *2*, 515.
(49) Fardad, M. A.; Yeatman, E. M.; Dawnay, E. J. C.; Green, M.; Horowitz, F. *J. Non-Cryst. Solids* **1995**, *183*, 260.
(50) Jasieniak, J.; Pacifico, J.; Signorini, R.; Chiasera, A.; Ferrari, M.; Martucci, A.; Mulvaney, P. *Adv. Funct. Mater.* **2007**, *17*, 1654.
(51) Van Embden, J.; Mulvaney, P. *Langmuir* **2005**, *21*, 10226.
(52) Van Embden, J.; Jasieniak, J.; Gomez, D. E.; Mulvaney, P.; Giersig, M. *Aust. J. Chem.* **2007**, *60*, 457.
(53) Jasieniak, J.; Fortunati, I.; Gardin, S.; Signorini, R.; Bozio, R.; Martucci, A.; Mulvaney, P. *Adv. Mater.* **2008**, *20*, 69.
(54) Xie, R.; Kolb, U.; Li, J.; Basche, T.; Mews, A. *J. Am. Chem. Soc.* **2005**, *127*, 7480.
(55) Garahan, A.; Pilon, L.; Yin, J.; Saxena, I. *J. Appl. Phys.* **2007**, *101*, 014320.
(56) Purcell, E. M. *Phys. Rev.* **1946**, *69*, 37.

JP106951Y